The Effect of Magnetically Induced Local Structure and Volume Fraction on the Electromagnetic Properties of Elastomer Samples with Ferrofluid Droplet Inserts

Catalin Nicolae Marin and Iosif Malaescu *

Posted Date: 1 December 2023

doi: 10.20944/preprints202312.0012.v1

Keywords: elastomer; ferrofluid; complex magnetic permeability; complex dielectric permittivity; electrical conductivity

Article

The Effect of Magnetically Induced Local Structure and Volume Fraction on the Electromagnetic Properties of Elastomer Samples with Ferrofluid Droplet Inserts

Catalin N. Marin [1] and Iosif Malaescu [1,2,*]

[1] West University of Timisoara, Dept. of Physics, Bd. V. Parvan no. 4, 300223 Timisoara, Romania; iosif.malaescu@e-uvt.ro; catalin.marin@e-uvt.ro;
[2] Institute for Advanced Environmental Research, West University of Timisoara (ICAM-WUT), Oituz Str., No. 4, 300086 Timisoara, Romania; iosif.malaescu@e-uvt.ro;
* Correspondence: iosif.malaescu@e-uvt.ro (I.M)

Abstract: Magnetic permeability (μ), dielectric permittivity (ε) and electrical conductivity (σ) of the six elastomer samples obtained by mixing silicone rubber (RTV-530) with a kerosene-based ferrofluid in different volume fractions, φ: 1.31%, 2.59% and 3.84%, were determined using the complex impedance measurements, over the frequency range (500 Hz-2 MHz). Three samples (A_0, B_0 and C_0) were manufactured in the absence of a magnetic field and the other three samples (A_h, B_h and C_h) in the presence of the magnetic field, H=43 kA/m. The component μ'' of the complex magnetic permeability of all samples presents a maximum, at a frequency f_{max}, which moves to higher values by increasing, φ, this maximum being attributed to Brownian relaxation processes. The conductivity spectrum, $\sigma(f)$ for all samples, follows the Jonscher universal law, which allows both the determination of the static conductivity σ_{DC}, and the barrier energy of electrical conduction process, W_m. For the same φ, W_m is lower and σ_{DC} is higher in the samples A_h, B_h and C_h than in the samples A_0, B_0 and C_0. The performed study is useful in manufacturing elastomers with predetermined properties and for possible applications, such as magneto-dielectric flexible electronic devices, which can be controlled by the volume fraction of particles or by an external magnetic field.

Keywords: elastomer; ferrofluid; complex magnetic permeability; complex dielectric permittivity; electrical conductivity

1. Introduction

A composite material is a system of two or more components with different properties, that are mixed to obtain a material with increased performance compared to its components. In recent years, there has been increasing interest in the research of composite materials with elastomers, to use them in various fields of science and technology [1–5].

A special interest has recently been observed for the development of multifunctional polymeric nanocomposites consisting of metal particles/oxides dispersed in a polymeric matrix [6]. The electrical properties of these composites depend on both the nature, size and concentration of the dispersed particles and the properties of the polymer matrix [7].

In the paper [8] the authors show that by the mixing of natural rubber (NR) with metal particles (Ni or Fe), elastomers with improved electrical and magnetic properties can be obtained. The epoxy composites filled with graphite nanoplatelets and magnetite [9] or with carbon nanotubes [10], represent new composite materials with important microwave properties. In recent years, another class of composites obtained by the combination of a silicone rubber with compounds of iron oxides has been much studied [11–13] and these composite materials, show excellent magneto-dielectric properties, useful in technological applications [14,15]. Also, an intensively studied fluidic composite is magnetic fluid or the ferrofluid, which is defined as a biphasic system of single-domain nanoparticles (Fe, Co, Fe_3O_4, Fe_2O_3, $CoFe_2O_4$, etc.) dispersed in a basic liquid and stabilized with a

 doi:10.20944/preprints202312.0012.v1

surfactant to prevent sedimentation [16]. On the other hand, the ferrofluid is considered a composite with magneto-dielectric properties, influenced by the presence of a magnetic field [17,18].

In this paper we reported the manufacture of six composite samples obtained by mixing silicone rubber (RTV-530) with a kerosene-based ferrofluid sample with magnetite particles in three volume fractions, φ (1.31%, 2.59% and 3.84%). For each volume fraction, φ, two samples were obtained, one polymerized in the presence of a static magnetic field, $H=43\ kA/m$ and another polymerized in the absence of the magnetic field. Based on the dynamic measurements over the range of 500 Hz - 2 MHz, the effect of volume fraction and of polymerization in magnetic field, on both of the complex magnetic permeability ($\mu=\mu'-i\mu''$) and complex dielectric permittivity ($\varepsilon=\varepsilon'-i\varepsilon''$) of the elastomer samples was investigated. The measurements of complex dielectric permittivity allowed the determination of the electrical conductivity (σ) of the manufactured samples. The obtained results were discussed considering the theoretical model CBH (*correlated barrier hopping*), being useful in possible technological applications.

2. Samples obtaining and characterization

Six elastomer type composite samples consisting of commercial RTV-530 silicone rubber (SR) from Prochima [19] having the density $\rho_{SR}=1.3\ g/cm^3$ and a kerosene-based ferrofluid (EFH 1 type from Ferrotech) [20], with magnetite particles, stabilized with oleic acid, having the density $\rho_{FM}=1.21\ g/cm^3$, were manufactured by mixing them. The silicone rubber has two components (A and B) being a non-toxic elastomer, with medium hardness and elasticity that can be used even as bolus material in radiotherapy [21].

In order to manufacture the composite samples, we mixed the same quantity M_{SR} of silicone rubber (equal quantities $M_{SR}/2$ of each component A and B) with a different quantity M_{FM} of ferrofluid, thus obtaining three samples, which differ by the volume fraction, φ of ferrofluid in the composite. The mixture thus formed was placed in a parallelepiped mold and pressed continuously for 2-3 minutes until it takes the shape of mold, and after 24 hours the composite samples are obtained, having the shape of a square parallelepiped plate with a side of 5 cm and a thickness of 0.1 cm. This polymerization/hardening of the sample mixture was done in the absence of the magnetic field, the composite samples obtained being denoted by sample A_0, sample B_0 and sample C_0. Also, three other composite samples having the same volume fractions φ, were polymerized in the presence of a magnetic field, $H=43\ kA/m$, being denoted by sample A_h, sample B_h and sample C_h.

The following quantities of materials were used to obtain the composite samples:

- for sample A_0 and A_h: $M_{FM}=0.05\ g$ and $M_{SR}=4\ g$ (2 g of each component of the silicon rubber, A and B);
- for sample B_0 and B_h: M_{FM} = 0.10 g and $M_{SR}=4\ g$ (2 g of each component of the silicon rubber, A and B);
- for sample C_0 and C_h: M_{FM} = 0.15 g and $M_{SR}=4\ g$ (2 g of each component of the silicon rubber, A and B).

Based on the density of the ferrofluid and of silicone rubber and their used mass, we have computed the total volume of the composite material: $V_{tot}=V_{SR}+V_{FM}$, and then the volume fraction, $\varphi = V_{FM} / V_{tot}$, of the ferrofluid in the composite samples. We obtained the following values: φ_1=1.31 %, φ_2=2.59 % and φ_3=3.84 %.

Figure 1 shows the optical microscopy images of the composite samples obtained both in the absence of the magnetic field (samples A_0, B_0 and C_0 in Figure 1 a), b) and c)) and in the presence of the magnetic field, H (samples A_h, B_h and C_h in Figure 1 d), e) and f)). As can be seen in Figure 1, when the sample preparation takes place in the presence of the magnetic field (Figs. 1 d), e) and f), the magnetite particles from ferrofluid tend to align on the direction of the field lines. forming parallel chains of particles, while in the absence of the magnetic field (Figs. 1 a), b) and c)), the particles are oriented randomly in the entire volume of the composite material observing the formation of particle agglomerations.

Preprints (www.preprints.org) | NOT PEER-REVIEWED | Posted: 1 December 2023 doi:10.20944/preprints202312.0012.v1

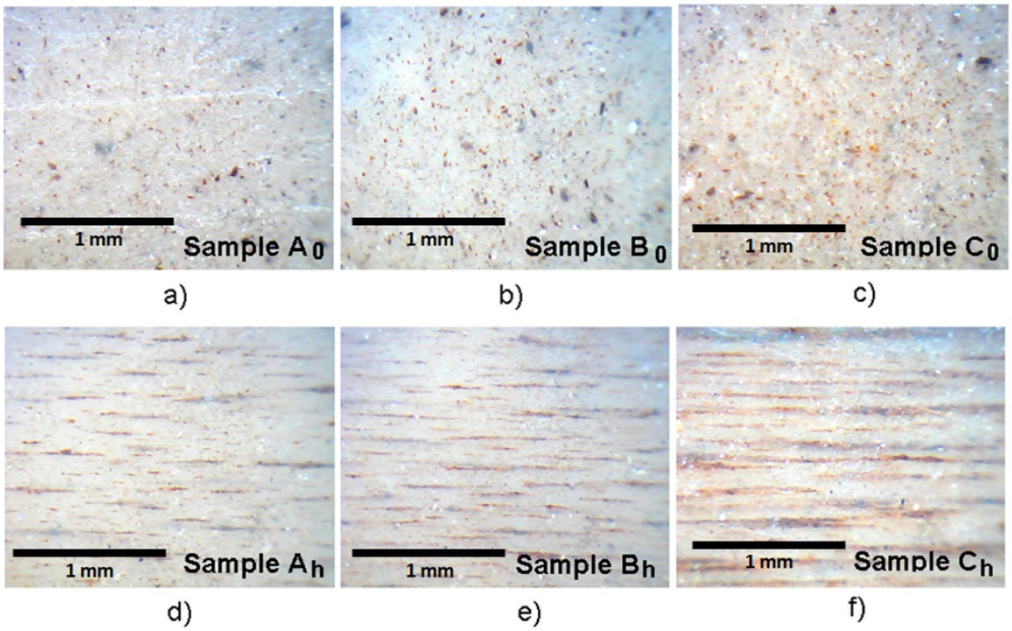

Figure 1. The images of the composite samples consisting of silicone rubber with ferrofluid: Samples A_0 (a), B_0 (b) and C_0 (c) obtained in the absence of magnetic field; samples A_h (d), B_h (e) and C_h (f) obtained in the presence of a magnetic field H=43 kA/m.

In Figure 2 is presented the static magnetization curve of the ferrofluid, used for the obtaining of the composite samples consisting of silicone rubber and ferrofluid. The curve, $M(H)$ was drawn by means of an induction hysteresis-graph [22] at low-frequency driving field (50 Hz).

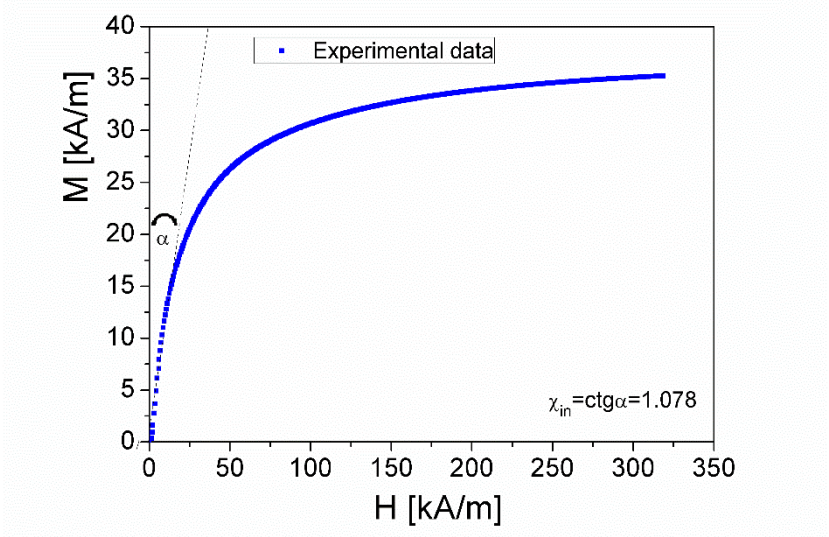

Figure 2. The dependence of the magnetization of ferrofluid, M, on the magnetic field, H.

As can be seen from Figure 2, the dependence of the magnetization, M, on the magnetic field, H, of the ferrofluid is of Langevin type, having a superparamagnetic behavior. From the experimental dependence $M(H)$ (Figure 2) and using the magneto-granulometry analysis of Chantrell [23], we have determined the following parameters of sample: the saturation magnetization (M_∞), the mean magnetic diameter of particles (d_m), the particle concentration (n) and the initial susceptibility (χ_{in}). The following values were obtained: M_∞=39.5 kA/m; d_m=11.74 nm; $n=10.49\cdot10^{22}$ m^{-3} and χ_{in}=1.078.

Preprints (www.preprints.org) | NOT PEER-REVIEWED | Posted: 1 December 2023 doi:10.20944/preprints202312.0012.v1

3. Results and discussion

3.1. Investigation of the complex magnetic permeability

The frequency dependence of real (μ') and imaginary (μ'') components of the complex magnetic permeability of the all samples, over the frequency range 500 Hz to 2 MHz was measured using an Agilent LCR-meter (E-4980A type) in conjunction with a coil containing the sample, by means of the following relationships [24]:

$$\mu' = \frac{X}{X_0} \qquad \mu'' = \frac{R - R_0}{X} \tag{1}$$

In Eq. (1), (R_0, X_0) and (R, X), represent the resistance and inductive reactance, measured with RLC-meter in the absence and in the presence of the sample inside the measuring coil, respectively. The obtained results for the composite samples are presented in Figure 3.

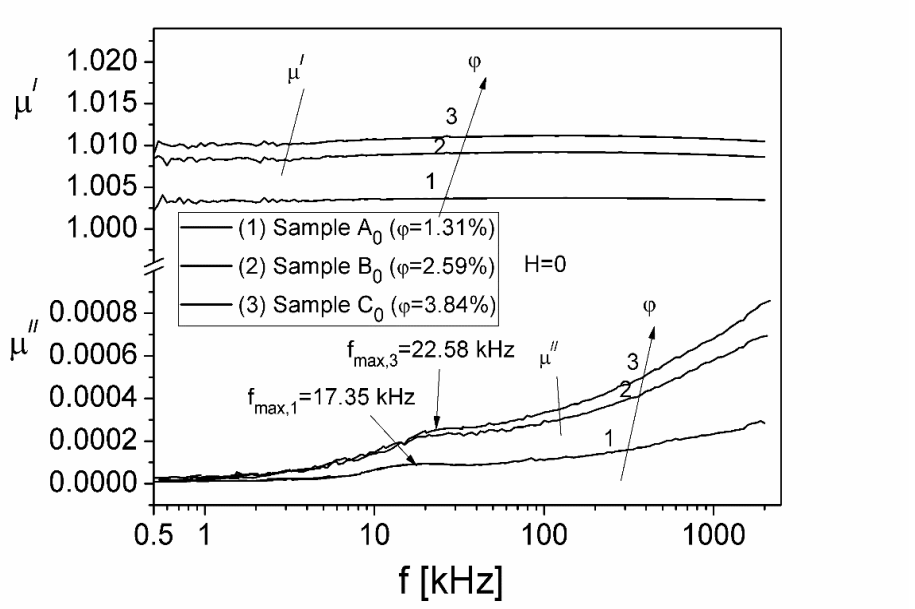

a)

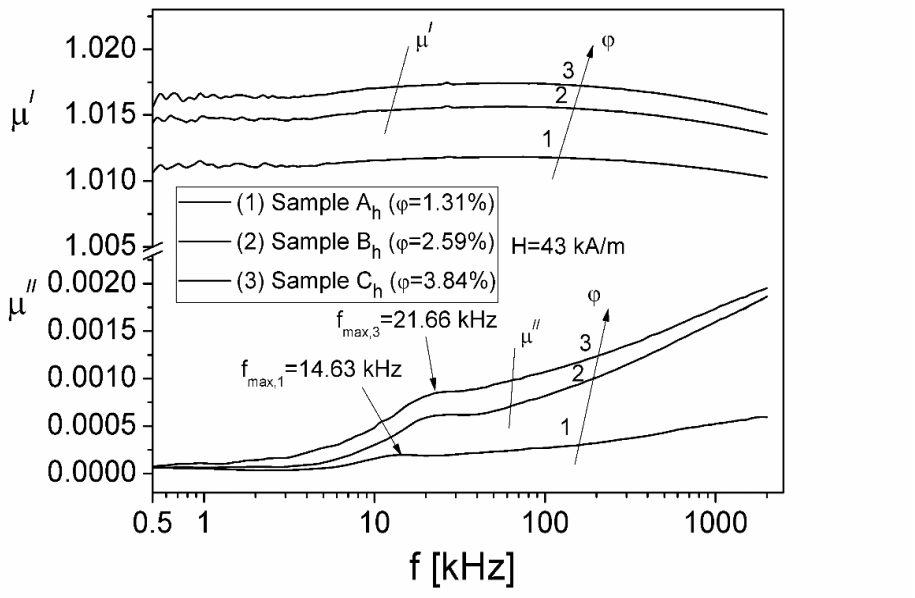

b)

Preprints (www.preprints.org) | NOT PEER-REVIEWED | Posted: 1 December 2023 doi:10.20944/preprints202312.0012.v1

Figure 3. The frequency dependence of the real, μ' and imaginary, μ'' components of the complex magnetic permeability of the: a) composite samples A_0, B_0 and C_0 and b) composite samples A_h, B_h and C_h.

From Figure 3 a) and b) it is observed that, at a constant value φ of the volume fraction, the real component, μ' of the complex magnetic permeability remains approximately constant with the frequency change. Also, for all samples, μ' increases by increasing the volume fraction, φ of the magnetite particles dispersed in the composite. It should be noted that the values μ' corresponding to samples A_h, B_h and C_h (Figure 3b)) obtained in the presence of the magnetic field H, are higher than those corresponding to samples A_0, B_0 and C_0 (Figure 3 a)), obtained in the absence of the magnetic field H, at all values φ of the volume fraction. This result shows that the preparation of such samples by mixing a ferrofluid with silicone rubber in the presence of an external magnetic field, H leads to obtaining composite samples with improved magnetic properties, that can be controlled by magnetic field, H and volume fraction, φ.

The imaginary component, μ'' of the complex magnetic permeability has a maximum (Figure 3) at a frequency f_{max}, for each composite sample, which moves to higher values of frequency by increasing the volume fraction, φ. The presence of maximum of $\mu''(f)$ means that all composite samples (A_0, B_0, C_0) and (A_h, B_h, C_h), exhibit a relaxation process in the investigated frequency range, characterized by a relaxation time, τ. From Debye's theory [25], it is known that the relaxation time τ is related to the frequency f_{max} at which μ'' is maximum, by the relation:

$$2\pi f_{\max}\tau = 1 \tag{2}$$

Considering the experimental values f_{max}, from Figs. 3 a) and b) and using Eq. (2), the corresponding values of the relaxation times were computed, resulting in the following values: $\tau_{(A0)}$=9.18 μs, $\tau_{(B0)}$=7.46 μs and $\tau_{(C0)}$=7.05 μs, for samples A_0, B_0 and C_0 and $\tau_{(Ah)}$=10.88 μs, $\tau_{(Bh)}$=7.96 μs and $\tau_{(Ch)}$=7.35 μs, for samples A_h, B_h and C_h, respectively. The dependence on the volume fraction, φ of the obtained relaxation times, τ is shown in Figure 4.

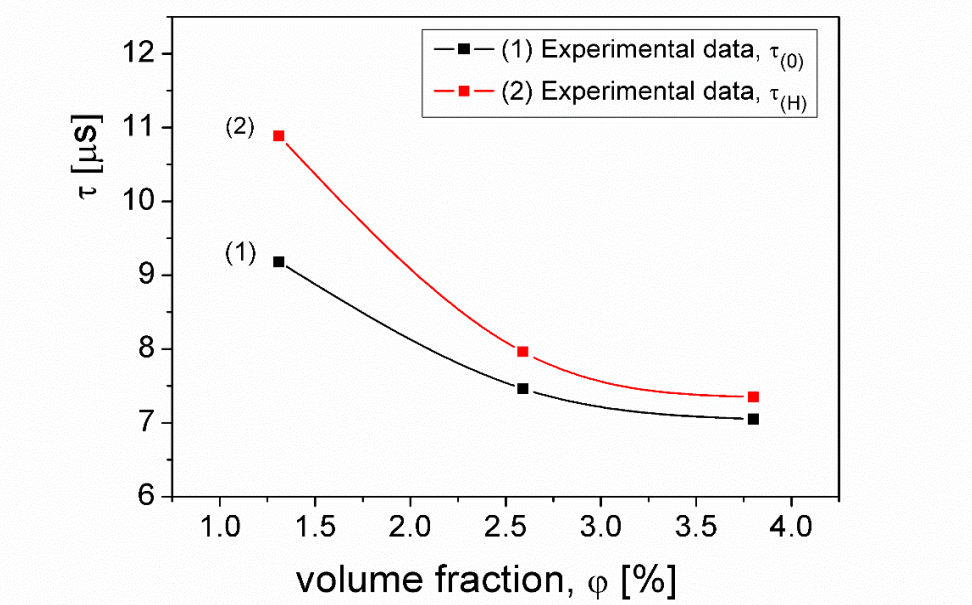

Figure 4. Volume fraction dependence of the relaxation times, $\tau(\varphi)$, for composite samples; $\tau_{(0)}$ – for samples A_0, B_0 and C_0, whilst $\tau_{(H)}$ – for the samples A_h, B_h and C_h. .

The obtained maxima of μ'', from Figs. 3 a) and b), could be attributed to either Néel relaxation process or to Brownian relaxation process. In the case of Neel relaxation process, the magnetic moments of the particles rotate inside the particles and the particles remain fixed in the composite [26], the relaxation time, τ_N is given by the relation:

Preprints (www.preprints.org) | NOT PEER-REVIEWED | Posted: 1 December 2023 doi:10.20944/preprints202312.0012.v1

$$\tau_N = \tau_0 \exp\left(\frac{KV_m}{kT}\right) \tag{3}$$

The Brownian relaxation process, is correlated to the particle's rotation, or rotation of particle aggregates, in the carrier liquid [26], being characterized by Brownian relaxation time τ_B and is given by the equation:

$$\tau_B = \frac{\pi\eta D_h^3}{2kT} \tag{4}$$

In the equations (3) and (4), K is the magnetocrystalline anisotropy constant of particles; V_m is the magnetic volume of a particle and τ_0 is a constant having the value 10^{-9} s [26,27]; k is the Boltzmann constant; T is the absolute temperature; η is the dynamic viscosity of the carrier liquid and D_h is the hydrodynamic diameter of the particle or the hydrodynamic diameter of the aggregate.

Assuming that the relaxation process is of Néel type and using the d_m value of the mean magnetic diameter of particles, obtained from the magnetization curve, d_m=*11.76 nm* (Figure 2), the anisotropy constant, K can be computed from Eq. (3) for all samples. The values found are: $K_{(A0)}=4.46\cdot10^4$ *J/m*^{3}, $K_{(B0)}=4.36\cdot10^4$ *J/m*^{3} and $K_{(C0)}=4.33\cdot10^4$ *J/m*^{3} for samples A_0, B_0 and C_0 and $K_{(Ah)}=4.54\cdot10^4$ *J/m*^{3}, $K_{(Bh)}=4.38\cdot10^4$ *J/m*^{3} and $K_{(Ch)}=4.35\cdot10^4$ *J/m*^{3} for samples A_h, B_h and C_h, respectively. These obtained values for the anisotropy constant K of the magnetite particles from the investigated composite samples are much higher than the values of the constant K which are in the range ($1.1\cdot10^4$ - $1.5\cdot10^4$) J/m^3 [28,29]. As a result, taking into account this result, it follows that the relaxation process corresponding to the maxima of the imaginary component μ'', from Figure 3, cannot be attributed to a Néel relaxation process.

If we assume that the relaxation process is Brownian, replacing in equation (4) the values of the relaxation time corresponding to all the investigated composite samples and considering the value $\eta=1.2\cdot10^{-3}$ *Pa·s*, for the viscosity of the carrier liquid (kerosene), we could determine the hydrodynamic diameter D_h of the particles in the samples. The values obtained are: $D_{h,A0}$=*27.13 nm*, $D_{h,B0}$=*25.32 nm* and $D_{h,C0}$=*24.84 nm* for the samples A_0, B_0 and C_0 and $D_{h,Ah}$=*28.71 nm*, $D_{h,Bh}$=*25.87 nm* and $D_{h,Ch}$=*25.20 nm*, for the samples A_h, B_h and C_h, respectively.

Figure 1 shows that the ferrofluid droplet inserts are present in all samples with the observation that for the samples polymerized in the magnetic field these inserts are elongated along the magnetic field lines. Therefore, the values determined for the hydrodynamic diameter D_h show that in all samples, aggregates of 2-3 particles rotate as a single structure in the carrier liquid of ferrofluid, within the droplet inserts from the composite. So, the maximum of the imaginary component μ'' from Figure 3 a) and b) is due to the Brownian relaxation process in the composite and that the ferrofluid droplet inserts are still present in the composite after polymerization.

3.2. Investigation of the complex dielectric permittivity

The real component, ε' and imaginary component, ε'' of the complex dielectric permittivity, were determined over the frequency range (500 Hz - 2 MHz). For this, each composite sample was placed in a planar capacitor with circular plates having the diameter of 4 cm and a distance between the plates, d=*1 mm*. The capacitor was connected to a RLC-meter. For a fixed frequency, f, the RLC-meter indicates the resistance, R and the reactance, X in the presence of the composite sample in the capacitor, respectively the resistance, R_0 and the reactance, X_0 in the absence of the sample in the capacitor. The components ε' and ε'' of the complex dielectric permittivity, were determined with the relations [30,31]:

$$\varepsilon' = \frac{X_0}{X} \qquad \varepsilon'' = X_0\left(\frac{1}{R} - \frac{1}{R_0}\right) \tag{5}$$

Figure 5 shows the frequency dependence of the real (ε') and imaginary (ε'') components, in the frequency range (500 Hz - 2 MHz) at different values of volume fraction, φ of particles.

Preprints (www.preprints.org) | NOT PEER-REVIEWED | Posted: 1 December 2023 doi:10.20944/preprints202312.0012.v1

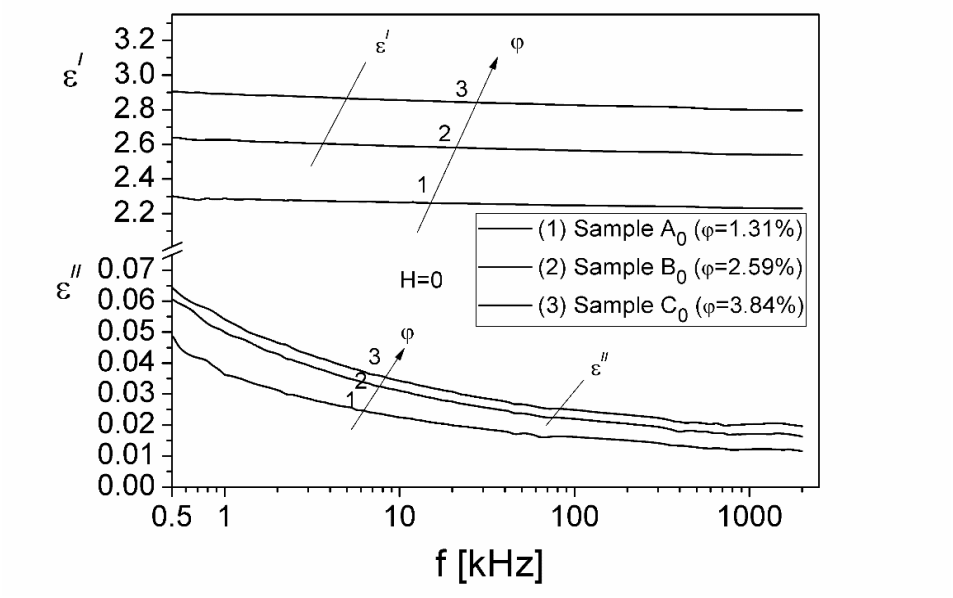

a)

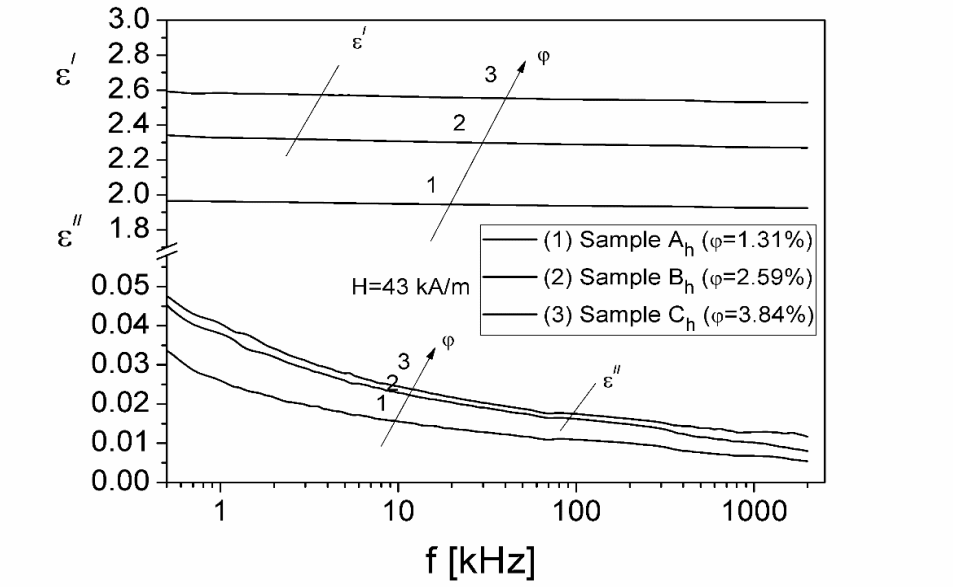

b)

Figure 5. The frequency dependence of the real, ε′ and imaginary, ε″ components of the complex dielectric permittivity of the: a) composite samples A_0, B_0 and C_0 and b) composite samples A_h, B_h and C_h.

As can be observed in figure 5 a) and b), at a constant value φ of the volume fraction, the real component ε′ of the complex dielectric permittivity remains approximately constant with the frequency change. Also, one can be observed that ε' increases from 2.3 to 2.9 (for samples A_0, B_0 and C_0, Figure 5 a)) and from 2.0 to 2.6 (for samples A_h, B_h and C_h Figure 5 b)), by increasing the volume fraction, φ, from 1.31% to 3.84%. The values ε' corresponding to samples A_h, B_h and C_h (Figure 5b)) obtained in the presence of the magnetic field H, are lower than those corresponding to samples A_0, B_0 and C_0 (Figure 5 a)), obtained in the absence of the magnetic field H, at all values, φ of the volume fraction.

For a constant value φ, of the volume fraction, the imaginary component ε'' of the complex dielectric permittivity decreases by increasing frequency, f, both for samples A_0, B_0 and C_0 and for samples A_h, B_h and C_h (Figure 5 a) and b)). Also, the values ε'' corresponding to samples A_h, B_h and

Preprints (www.preprints.org) | NOT PEER-REVIEWED | Posted: 1 December 2023 doi:10.20944/preprints202312.0012.v1

C_h (Figure 5 b)) are smaller than those corresponding to samples A_0, B_0 and C_0 at any frequency *f* and the same value of the volume fraction, φ.

This result shows that the preparation of such samples by mixing a ferrofluid with silicone rubber, in the presence of an external magnetic field, leads to obtaining of composite samples with different dielectric properties, that can be controlled by the magnetic field, *H* and by the volume fraction, φ.

3.3. DC and AC conductivity

It is known that, for the study of composite materials, an important parameter is the electrical conductivity, σ, which can be determined from the dielectric data of permittivity [32,33] with relation:

$$\sigma = 2\pi f \varepsilon_0 \varepsilon'' \tag{6}$$

The conductivity σ, provides information about the transport of electric charge in materials [33,34], being useful for different applications. Based on the experimental values ε'' of the complex dielectric permittivity (Figure 5 a) and b)), the electrical conductivity, σ, of the composite samples was determined with the equation (6). The frequency dependence of the conductivity, σ, in the frequency range 500 Hz - 2 MHz, is shown in Figure 6 a) for samples A_0, B_0 and C_0 and in Figure 6 b) for samples A_h, B_h and C_h.

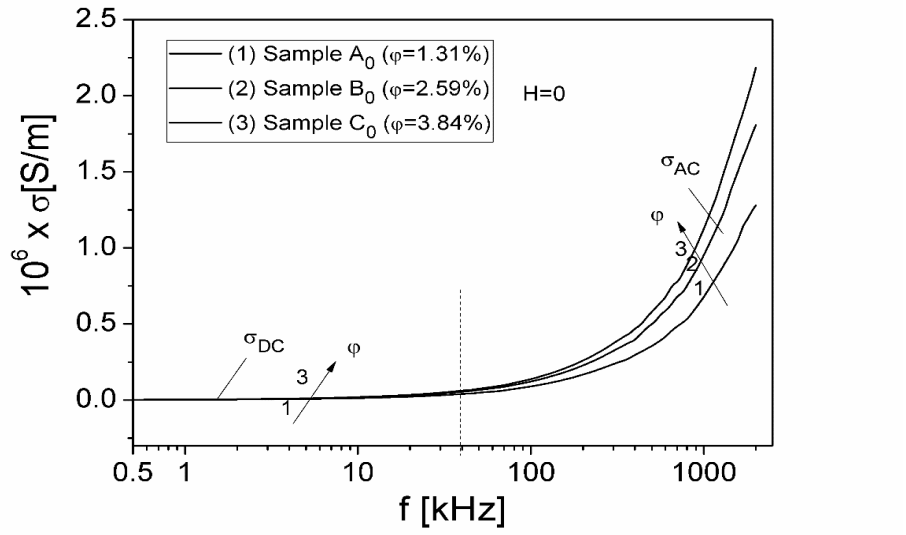

a)

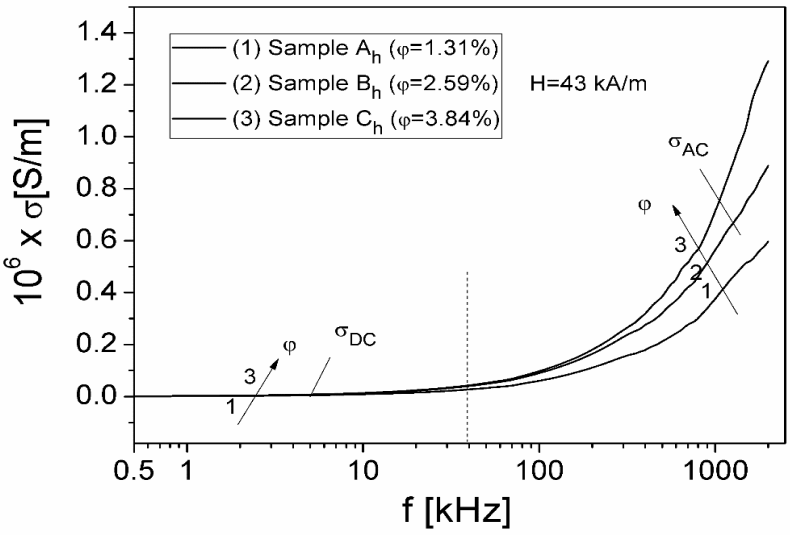

b)

Preprints (www.preprints.org) | NOT PEER-REVIEWED | Posted: 1 December 2023 doi:10.20944/preprints202312.0012.v1

Figure 6. The frequency dependence of the conductivity, σ, of the samples A_0, B_0 and C_0 (a) and and A_h, B_h and C_h (b).

From figure 6, it is observed that the conductivity spectrum, $\sigma(f)$, presents two regions: 1) a region in which σ remains constant with the frequency, corresponding to DC-conductivity (σ_{dc}) and 2) a dispersion region, where σ depends on frequency, corresponding to AC-conductivity (σ_{ac}). In other papers [9,35], a similar conductivity frequency dependence was obtained for other composite samples obtained by the combination of the Fe_3O_4 nanoparticles or graphite nanoplatelets with a polymer. This frequency behavior of the electrical conductivity from Figure 6, of the elastomer composite samples, agrees with the Jonscher universal law [36]:

$$\sigma(\omega) = \sigma_{DC} + \sigma_{AC} \tag{7}$$

The values of static conductivity σ_{DC} remain approximately constant with frequency, up to about 30 kHz, for each volume fraction φ, both for the composite samples A_0, B_0 and C_0 (Figure 6 a)) and for the samples A_h, B_h and C_h (Figure 6 b)), the σ_{DC} obtained values being listed in Table 1.

Table 1. The parameters of composite samples determined from measurements.

Samples	**A_0**	**B_0**	**C_0**	**A_h**	**B_h**	**C_h**
	φ=1.31%	***φ=2.59%***	***φ=3.84%***	***φ=1.31%***	***φ=2.59%***	***φ=3.84%***
Parameters		***H=0***			***H=43 kA/m***	
σ_{DC} [S/m]	$4.26 \cdot 10^{-9}$	$9.40 \cdot 10^{-9}$	$1.03 \cdot 10^{-8}$	$4.93 \cdot 10^{-9}$	$1.73 \cdot 10^{-8}$	$1.86 \cdot 10^{-8}$
n	0.897	0.915	0.938	0.751	0.807	0.872
A [S/m]	$5.42 \cdot 10^{-13}$	$5.72 \cdot 10^{-13}$	$4.73 \cdot 10^{-13}$	$28.7 \cdot 10^{-13}$	$20.4 \cdot 10^{-13}$	$8.56 \cdot 10^{-13}$
W_m [eV]	1.51	1.83	2.51	0.62	0.81	1.22

From Table 1, it is observed that by increasing the volume fraction φ of particles, the σ_{DC} conductivity increases for all composite samples. Also, the values of σ_{DC} corresponding to samples manufactured in the presence of magnetic field (samples A_h, B_h and C_h) are higher than the σ_{DC} values of samples A_0, B_0 and C_0, manufactured in the absence of the magnetic field. Therefore, the σ_{DC} conductivity of composite samples is correlated with the sample manufacturing process. When sample preparation takes place in the presence of the magnetic field, the magnetite particles from ferrofluid align in the direction of the magnetic field, forming parallel chains of particles (see Figure 1 d), e) and f), which leads to an increase in the conductivity σ_{DC}, in relation to σ_{DC} of the samples prepared in the absence of magnetic field when the particles are randomly oriented in the entire volume of the elastomer composite material (see Figure 1 a), b) and c)).

The component σ_{AC} of the conductivity depends on the frequency, being correlated with the dielectric relaxation processes due to the localized electric charge carriers from the composite samples and is given by the following equation:

$$\sigma_{AC} = A\omega^n \tag{8}$$

where n is an exponent which is dependent on both frequency and temperature ($0 < n < 1$) and A is a pre-exponential factor [37].

The logarithmation of equation (8) leads to a linear dependence between $ln\sigma_{AC}$ and $ln\omega$, which is shown in Figure 7 a) for samples A_0, B_0 and C_0 and in Figure 7 b) for samples A_h, B_h and C_h, respectively. Fitting the experimental dependencies, $ln(\sigma_{AC})(ln(\omega))$, from Figure 7 a) and b), with a straight line, we determined the exponent n and the parameter A, corresponding to all the values of the volume fraction, φ. The values obtained are listed in Table 1. It is observed that the values of exponent n, corresponding to samples A_h, B_h and C_h, obtained in the presence of a magnetic field H, are lower than the values n corresponding to samples A_0, B_0 and C_0, for the same value φ of the volume fraction.

To investigate the electrical conduction mechanism in an elastomeric composite sample, several theoretical models [38,39] can be applied, such a commonly used model being the correlated barrier

Preprints (www.preprints.org) | NOT PEER-REVIEWED | Posted: 1 December 2023 doi:10.20944/preprints202312.0012.v1

hopping (CBH) theoretical model [39]. According to the CBH model, the exponent n can be written in a first approximation as [39]:

$$n = 1 - \frac{6kT}{W_m} \tag{9}$$

In Eq. (9), W_m represents the barrier energy [39,40]. Using the relation (9), and the values, n, we determined the barrier energy of electrical conduction process of each investigated sample. The obtained results for W_m are shown in Table 1.

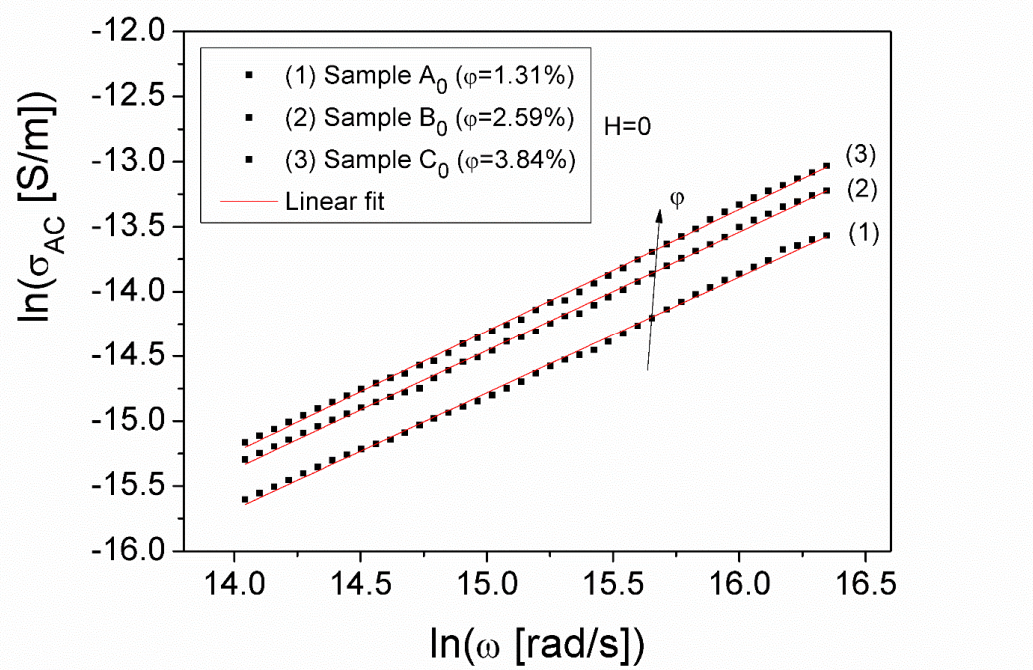

a)

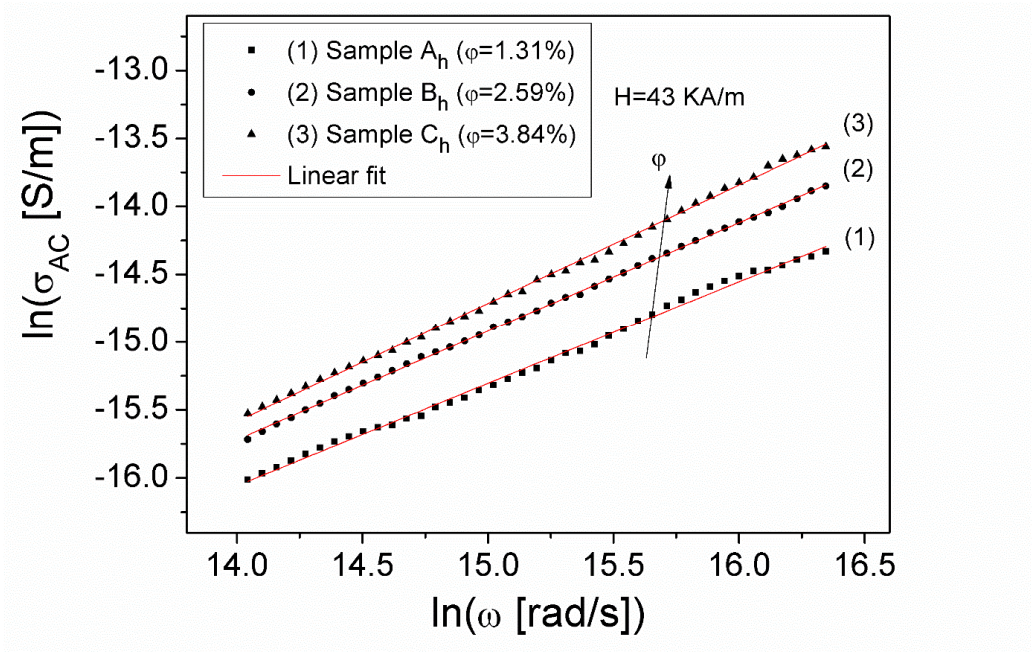

b)

Figure 7. The $ln\sigma_{ac}(ln\omega)$ dependence for composite samples A_0, B_0 and C_0 (a) and samples A_h, B_h and C_h, respectively (b).

 doi:10.20944/preprints202312.0012.v1

As can be seen from Table 1, the increase in the volume fraction φ of the particles leads to an increase in the barrier energy W_m for all composite samples. Also, the W_m values corresponding to the samples manufactured in the presence of the magnetic field (samples A_h, B_h and C_h) are lower than the W_m values of the samples A_0, B_0 and C_0, manufactured in the absence of the magnetic field. Therefore, the decrease of the barrier energy W_m of samples A_h, B_h and C_h, compared to the barrier energy of samples A_0, B_0 and C_0, will lead to an increase in the number of charge carriers that will be able to participate in the electrical conduction in these samples, which determines an increase in their conductivity, as we obtained experimentally (see Table 1).

4. Conclusions

In this paper, six composite samples have been manufactured both in absence and in the presence of a magnetic field, by mixing the silicone rubber (RTV-530) with a kerosene-based ferrofluid with magnetite particles, in different volume fractions of particles φ (1.31%, 2.59% and 3.84%). Based on the complex impedance measurements, in low frequency field between, over the range (0.5 kHz - 2 MHz), the complex magnetic permeability $\mu=\mu'-i\mu''$, the complex dielectric permittivity $\varepsilon=\varepsilon'-i\varepsilon''$ and electrical conductivity, σ, of all composite samples were determined. The obtained results for the complex magnetic permeability of the elastomeric composite samples, show that the imaginary component μ'' has a maximum, at low frequencies between (0.1 - 0.3) kHz, both for samples manufactured in absence of magnetic field (samples A_0, B_0 and C_0) and for samples manufactured in presence of a magnetic field, H (samples A_h, B_h and C_h). This maximum is attributed to Brownian relaxation process within the ferrofluid droplet inserts from the composites. Using the experimental results of the complex dielectric permittivity, the conductivity spectra, $\sigma(f)$ for all investigated samples, were determined. The spectra $\sigma(f)$ obeys the Jonscher universal law, having two regions: a region in which σ does not vary with frequency, corresponding to DC-conductivity (σ_{DC}) and a dispersion region, where σ rapidly increases with frequency, corresponding to AC-conductivity (σ_{AC}). The increase of the volume fraction of particles in elastomeric composite samples, from φ=1.31 % to x=3.84 %, leads to the increase of σ_{DC} from $4.26\cdot10^{-9}$ S/m to $1.03\cdot10^{-8}$ S/m for the samples A_0, B_0 and C_0 and from $4.93\cdot10^{-9}$ S/m to $1.86\cdot10^{-8}$ S/m for the samples A_h, B_h and C_h, respectively. Based on the Jonscher universal response and on the CBH (correlated barrier hopping) theoretical model, we evaluated for all composite samples the energy barrier of the electrical conduction process, W_m. The results show that the W_m values corresponding to the samples manufactured in the presence of the magnetic field (samples A_h, B_h and C_h) are lower than the W_m values of the samples A_0, B_0 and C_0 manufactured in the absence of the magnetic field, for all values φ of the volume fraction, this result agreeing with the increase of their conductivity, σ_{DC}. The results obtained are very useful for the manufacture of elastic composites with predetermined properties, that can be tuned by the change of volume fraction of particles inside the composite or by modifying the local structure, in the presence of an external magnetic field.

Author Contributions: Conceptualization, I.M. and C.N.M.; methodology, I.M.; software, C.N.M.; validation, I.M. and C.N.M.; formal analysis, C.N.M.; resources, C.N.M. and I.M.; investigation, C.N.M.; writing—original draft preparation, I.M.; writing—review and editing, C.N.M. and I.M.; visualization, I.M. and C.N.M.; supervision, C.N.M. and I.M. All authors have read and agreed to the published version of the manuscript.

Institutional Review Board Statement: Not applicable.

Data Availability Statement: Data will be made available on request.

Conflicts of Interest: The authors declare no conflict of interest.

References

1. Choi, S.; Han, S.I.; Kim, D.; Hyeon, T.; Kim, D.H. High-performance stretchable conductive nanocomposites: materials, processes, and device applications. *Chem. Soc. Rev.* **2019**, *48*, 1566–1595.
2. Wang, B.; Thukral, A.; Xie, Z.; *et al.* Flexible and stretchable metal oxide nanofiber networks for multimodal and monolithically integrated wearable electronics. *Nat. Commun.* **2020**, *11(1)*, 2405-2420.

3. Cao, J.; Ling, Z.; Lin, X.; Wu, Y.; Fang, X.; Zhang, Z. Flexible composite phase change material with enhanced thermophysical, dielectric, and mechanical properties for battery thermal management, J. Energy Stor. **2022**, 52, Part A, 104796.
4. Namkoong, M.; Guo, H.; Rahman, M.S.; *et al.* Moldable and transferable conductive nanocomposites for epidermal electronics. *npj Flex Electron*. **2022**, 6(41), 1-9.
5. Zhang, C.; Liu, S.; Wei, F.; Dong, L.; Zhao, D.; Ou, Y. Magnetodielectric Properties of Ordered Microstructured Polydimethylsiloxane-Based Magnetorheological Elastomer with Fe_3O_4@rGO Nanoparticles. *Polymers*. **2023**, *15*, 941.
6. Kurahatti, R.V.; Surendranathan, A.O.; Kori, S.A.; Singh, N.; Ramesh Kumar, A.V.; Srivastava, S. Defence applications of polymer nanocomposites. *Def. Sci. J.* **2010**, 60, 551e563.
7. Hammami, H; Arous, M.; Lagache Mand Kallel, A. Study of the interfacial MWS relaxation by dielectric spectroscopy in unidirectional PZT fibres/epoxy resin composites, *J. Alloys. Compd.* **2007**, 430, 1–8.
8. Jamal, E.M.A.; Joy, P.A.; Kurian, P.; Anantharaman, M.R. Synthesis of nickel-rubber nanocomposites and evaluation of their dielectric properties, *Mat. Sci. Eng. B*. **2009**, 156, 24-31.
9. Yakovenko, O.S.; Yu. L.; Matzui, L.; Vovchenko, L.; Lozitsky, O.V.; Prokopov, O.I.; Lazarenko, O.A.; Zhuravkov, A.V.; Oliynyk, V.V.; Launets, V.L.; Trukhanov, S.V.; Trukhanov, A.V. Electrophysical properties of epoxy-based composites with graphite nanoplatelets and magnetically aligned magnetite, *Molec. Cryst. Liq. Cryst.* **2018**, 661, 68-80.
10. Yakovenko, O.S.; Yu. L.; Matzui, L.; Vovchenko, L.; Oliynyk, V.V.; Trukhanov, A.V.; Trukhanov, S.V.; Borovoy, M.O.; Tesel'ko, P.O.; Launets, V.L.; Syvolozhskyi, O.A.; Astapovich, K.A. Effect of magnetic fillers and their orientation on the electrodynamic properties of $BaFe_{12-x}Ga_xO_{19}$ (x = 0.1–1.2)—Epoxy composites with carbon nanotubes within GHz range, *Appl. Nanosci.* **2020**, 10, 4747-4752.
11. Bica, I. The obtaining of magneto-rheological suspensions based on silicon oil and iron particles, *Mat. Sci. Eng.: B*. **2003**, 98(2), 89-93.
12. Bunoiu, M.; Bica, I. Magnetorheological elastomer based on silicone rubber, carbonyl iron and Rochelle salt: Effects of alternating electric and static magnetic fields intensities. *J. Ind. Eng. Chem.* **2016**, 37, 312-318.
13. Bica, I.; Anitas, E.M.; Averis, L.M.E.; Bunoiu, M. Magnetodielectric effects in composite materials based on paraffin, carbonyl iron and graphene. *J. Ind. Eng. Chem*. **2015**, 21, 1323-1327.
14. Vinnik, D.A.; Podgornov, F.V.; Zabeivorota, N.S.; Trofimov, E.A.; *et. al*. Effect of treatment conditions on structure and magnetodielectric properties of barium. *J. Magn. Magn. Mater*. **2020**, 498, 166190.
15. Kozlovskiy, A.L.; Kenzhina, I.E.; Zdorovets, M.V. $FeCo–Fe_2CoO_4/Co_3O_4$ nanocomposites: Phase transformations as a result of thermal annealing and practical application in catalysis**.** *Ceram. Int*. **2020,** 46(8), Part. A, 10262-10269.
16. Rosensweig, R.E. *Ferrohydrodynamics*, Cambridge University Press, 1985.
17. Fannin, P.C.; Marin, C.N.; Malaescu, I. The Influence of Particle Concentration and Polarizing Field on the Resonant Behaviour of Magnetic Fluids. *J. Phys. Condensed Matter*. **2003**, 15(27), 4739–4750.
18. Fannin, P.C.; Malaescu, I.; Marin, C.N. Determination of the Landau–Lifshitz damping parameter of composite magnetic fluids. *Phys. B*. **2007**, 388, 93–98.
19. **** http://www.prochima.com/ENG/product.asp?id=7
20. **** https://ferrofluid.ferrotec.com/products/ferrofluid-educational-fluid/efh/efh1/
21. Spunei, M; Malaescu, I.; Mihai M.; Marin, C.N. Absorbing materials with applications in radiotherapy and radioprotection. *Rad. Prot. Dosim*. **2014**, 162(1-2), 167-170.
22. Ercuta, A. Sensitive AC hysteresigraph of extended driving field capability, *IEEE Trans. Instrum. Measur*. **2020**, 69(4), 1643–1651.
23. Chantrell, R.W.; Popplewell, J.; Charles, S.W. Measurements of particle size distribution parameters in ferrofluids. *IEEE Trans. Magn*. **1978**, 14, 975.
24. Malaescu, I.; Fannin, P.C.; Marin, C.N.; Lazic, D. The concept of ferrofluid preheating in the treatment of cancer by magnetic hyperthermia of tissues, *Med. Hypoth.* **2018**, 110, 76-79.
25. Debye, P. *Polar Molecules*, The Chemical Catalog Company, New York, 1929.
26. Odenbach, S. *Ferrofluids*, 594, Springer, Berlin Heidelberg, 2002.
27. Fannin, P.C.; Charles, S.W. The study of a ferrofluid exhibiting both Brownian and Neel relaxation. *J. Phys. D, Appl. Phys*. **1989**, 22, 187-191.
28. Bickford, L.R. Ferromagnetic Resonance Absorption in Magnetite Single Crystals. *Phys. Rev.* **1950**, 78, 449.
29. Malaescu, I.; Marin, C.N. Study of magnetic fluids by means of magnetic spectroscopy, *Phys. B: Cond. Matter*. **2005**, 365, 134-140.
30. Lungu, A.; Malaescu, I.; Marin, C.N.; Vlazan, P.; Sfirloaga, P. The electrical properties of manganese ferrite powders prepared by two different methods. Phys. B. **2015**, 462, 80-85.
31. ASTM D150-98 - Standard test methods for AC loss characteristics and permittivity (dielectric constant) of solid electrical insulation.
32. Scaife, B.K.P. *Principles of Dielectrics*, Oxford Clarendon Press, 1998.

33. Marin, C. N.; Fannin, P.C.; Malaescu, I.; Matu, G. Macroscopic and microscopic electrical properties of a ferrofluid in a low frequency field. *Phys. Lett. A*. **2020**, 384, 126786.
34. Yakovenko, L.; Matzui, Y.; Vovchenko, L.L.; Lozitsky, O.V.; Prokopov, O.I.; Lazarenko, O.A.; Zhuravkov, A.V.; Oliynyk, V.V.; Launets, V.L.; Trukhanov, S.V.; Trukhanov, A.V. Electrophysical properties of epoxy-based composites with graphite nanoplatelets and magnetically aligned magnetite. *Molec. Cryst. Liq. Cryst*. **2018**, 661, 68-80.
35. Trukhanov, A.V.; Algarou, N.A.; Slimani, Y.; Almessiere, M.A.; Baykal, A.; Tishkevich, D.I.; Vinnik, D.A.; Vakhitov, M.G.; Klygach, D.S.; Silibin, M.V.; Zubar, T.I.; Trukhanov, S.V. Peculiarities of the microwave properties of hard–soft functional composites $SrTb_{0.01}Tm_{0.01}Fe_{11.98}O_{19}$– AFe_2O_4 (A = Co, Ni, Zn, Cu, or Mn). *RSC Adv*. **2020**, 10, 32638.
36. Jonscher, A.K. *Universal Relaxation Law*, 1st edn.: Chelsea Dielectrics Press: London, 1996.
37. Funke, K. Prog. Jump relaxation in solid electrolytes Solid State Chem. **1993**, 22, 111-195.
38. Okuda, T.; Jufuku, N.; Hidaka, S.; Terada, N. Magnetic, transport, and thermoelectric properties of the delafossite oxides $CuCr_{1-x}Mg_xO_2$ ($0 \leqslant x \leqslant 0.04$). *Phys. Rev. B*. 2005, 72, 144403.
39. Pike, G. E. AC conductivity of scandium oxide and a new hopping model for conductivity. *Phys. Rev. B*. **1972**, 6, 1572-1580.
40. Elliott, S.R.; A theory of ac conduction in chalcogenide glasses. *Philos. Mag. B*. **1977**, 36(6), 1291-1304.